# Estimating wind power production loss due to icing

Ø. Byrkjedal, PhD
Kjeller Vindteknikk AS
P.O.Box 122, N-2027 Kjeller, Norway, oyvind.byrkjedal@vindteknikk.no

**A meso-scale model has been used to develop regional wind resource maps in Norway on a 1km * 1km horizontal grid. The results from the simulations have also been used to develop icing maps for the same regions.**

**The degree of icing is found to be strongly dependent on elevation, but also to depend on wind speed and wind direction. For a location in northern Norway we find a tendency that icing is more likely to occur in combination with higher than with lower wind speeds.**

**Expected production has been calculated by combining the simulated wind speed with the power curve of a chosen turbine. By the use of different methodologies, the icing calculations have been used to estimate production losses due to in-cloud icing.**

## I. Introduction

THE WRF model makes a promising tool for wind resource mapping. The model results with regard to wind speed have been validated in e.g. [1], [2] and [3]. Combined with wind measurements at various locations, we can use this tool to locate good sites to develop wind power. A regional wind resource map of southwestern Norway is presented in [3].

Icing can be a challenge to wind power at high altitudes in general and also at lower altitudes in Northern Europe. Moisture combined with temperature below freezing during winter makes icing on wind turbines a potential problem in Northern Europe. Icing on wind turbines reduces the power output at any wind speed, and can also be associated with larger wear/stress of the gearbox, generator and rotor blades.

The frequency and severity of icing episodes are strongly dependent upon the site's elevation above sea level. But areas at higher elevation are also typically the sites with the best wind resources. In order to exploit the best wind resources one needs also consider the challenges due to icing, and the related production losses to be expected at such sites.

## II. Models

### A. *The WRF model and setup*

The Weather Research and Forecast (WRF) model is a next generation meso-scale numerical weather prediction system, aiming at both operational forecasting and atmospheric research needs. A description of the modeling system can be found at the home page http://www.wrf-model.org/. Details about the modeling structure, numerical routines and physical packages available can be found in for example [4] and [5].

WRF solves coupled equations for all important physical processes (such as winds, temperatures, stability, clouds, radiation etc.) in the atmosphere based on the initial fields and the lateral boundary values derived from the global data. The WRF-model calculates the change in the meteorological fields for each grid-cell for a time step of five seconds. Thus a realistic temporal development of the meteorological variables is achieved.

The model is set up with two 2-way nested model domains shown in Fig. 1. We use a horizontal resolution of 5 km for the outer domain and 1 km for the inner domain. We use 32 layers vertically, with the lowest 4 model levels at 20 m, 60 m, 115 m and 190 m above the ground. The model is run for one full year, the period 01.01.2005 – 31.12.2005.

The analysis in this paper will focus on the southern part of the inner model domain.

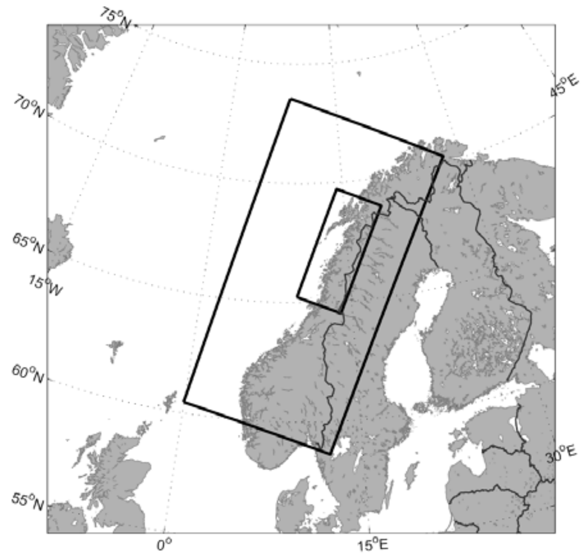


Fig. 1. Inner and outer domain of the WRF-calculations for Nordland

### B. *Icing calculations*

According to [6] icing has been calculated from:

$$\frac{dM}{dt} = \alpha_1 \alpha_2 \alpha_3 \cdot w \cdot A \cdot V \qquad (1)$$

Here dM/dt is the icing rate on a standard body (defined by [6] as a cylinder of 1m length and diameter 30mm). w is the liquid water content, A is the collision area perpendicular to the flow of air. V is the collision speed. $\alpha_1$, $\alpha_2$ and $\alpha_3$ are the collision efficiency, sticking efficiency and accretion efficiency.

The collision efficiency, $\alpha_1$, is an estimate of the number of droplets that collide with the object. The value is given as a ratio in the range 0 to 1. $\alpha_1$ depends on the collision speed, collision area, shape of the object and the size of the droplets. $\alpha_1$ is described by an empiric formulation as given in [6].

The sticking efficiency, $\alpha_2$, estimates the number of droplets that collide with the object that will stick to the object given as a ratio. For super cooled droplets the sticking efficiency will be close to 1.

When a droplet hits the object and freezes, latent freezing energy is released from the droplet. For temperatures close to 0°C there may be too little cooling of the water before it is blown off. The accretion efficiency, $\alpha_3$, can be reduced from 1 for temperatures close to 0°C. The formulation of $\alpha_3$ is given in [6].

An icing episode is identified from the model data when the icing rate (dM/dt) comes above 10g/hour, which is equivalent to a 0.5mm layer of ice on the standard body.

## III. Results

The wind resource map at 80m height as calculated from the model simulations is shown in Fig. 2. Comparisons have been performed between the model and wind speed measured at heights ranging from 10m to 100m height by [1]-[3]. It has been found that the annual average wind speed calculated by the model typically lies within 10% of the observed value. The results show that the model uncertainties are larger for areas with complex terrain than for areas with less terrain complexity. The correlation coefficient, R, between hourly values of modeled versus observed wind speed is typically in the range 0.7-0.9. The wind direction calculated from the model fits the observed distribution quite well.

A map showing the icing conditions calculated from the model results using (1) is presented in Fig. 3. The map shows the number of occurrences when we find dM/dt > 10g/hr during 1 year of model data. Icing has been calculated for the WRF grid at all model levels. The icing amounts are very dependent on height. Therefore the icing levels have been adjusted by employing a fine scale topography mesh with horizontal resolution of 25m (N50 topography) to adjust for the smoothed WRF topography (1km).

Reference [3] has compared icing calculated from model results and finds a good correlation between the statistical properties of icing episodes found from the model and calculations based on cloud height observations from airports in Norway. The validation is further refined in [7] by comparing WRF output icing data to icing data generated from airport cloud, temperature, and wind data and the common icing accumulation equation (1). The two methods produce results in excellent agreement.

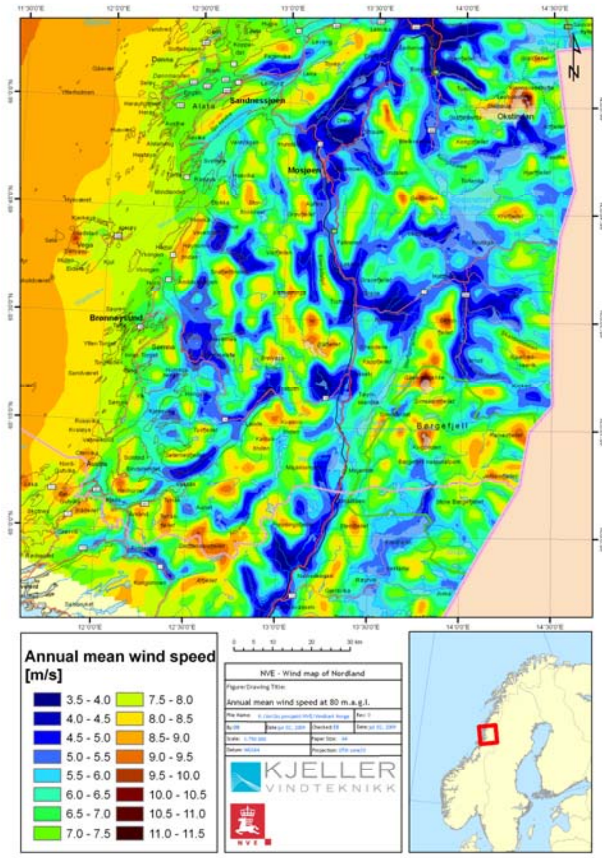


Fig. 2. Expected annual mean wind speed at 80m height.

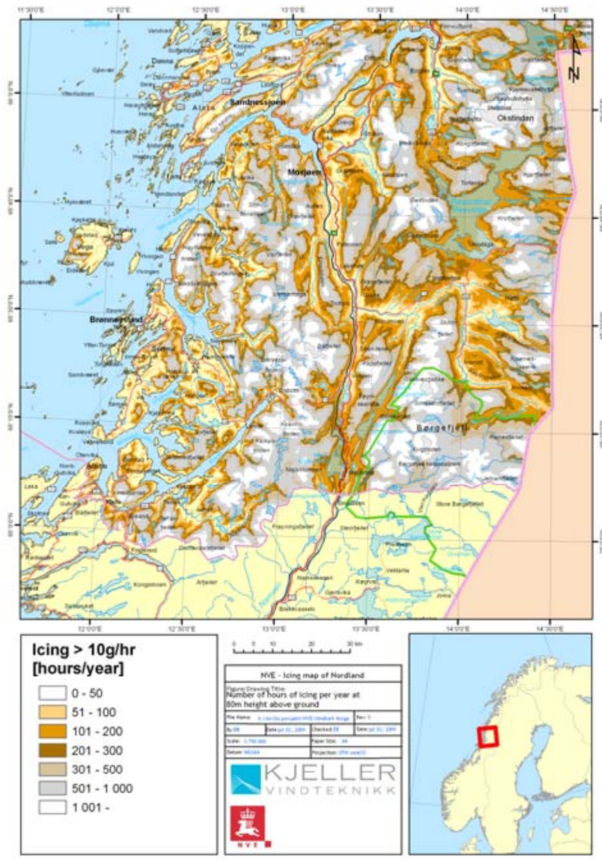


Fig. 3. Number of hours per year with ice accumulation

## IV. Estimating Production Loss

Ice on the rotor blades will affect the performance of a wind turbine. Ice on the blades modifies the aerodynamic properties of the blade resulting in lower production [8]-[9]. Also instruments on the turbine will experience icing which may cause the turbine to shut down.

We here define any period when the icing rate is greater than 10g/hr as an icing event. During all icing events ice will accumulate on the standard body. Production loss is in this paper estimated by assuming that the turbine will shut down during all icing events. Further when the icing event is over (icing rate becomes lower than 10g/hr). This is a relatively simple approach to estimate production losses. But since the experience with running wind turbines during icing conditions with iced blades is limited or not available from the operators, this seems to be a reasonable approach.

A rotating blade will accumulate more ice than a stationary blade. To stop production during the icing events should be done to avoid heavy ice loads. Further we assume that the production will continue as normal (with clean blades) when the icing episode has finished. This implies some sort of de-icing system or that any ice loads is removed mechanically. The cost of running a de-icing system is not considered in this paper.

The distribution of wind speed and wind direction for an exposed site in Nordland in Northern Norway is shown in Fig. 4 and Fig. 5 The site is located at 770 meters above sea level and is found from Fig. 3 to experience 1000 hours of icing. For wind speed we find that the frequency distribution for the cases with icing differs from the site's Weibull distribution, icing is more common at higher wind speeds. The modal value of the wind speed distribution at this location is 4 m/s while for the cases with icing the modal value is 7 m/s. From Fig. 5 we find that it is wind from sectors 8-11 (from southwest to northwest) that contribute the most to icing at this site. This corresponds to the direction of the water source, and also to the main wind directions at this site. The relative maximum is found for sector 9 where 23% of the cases with wind from this direction are related to icing. Calculating the production loss using time series of wind speed and icing, and assuming no production during icing events we estimate the production loss to be 22%.

Assuming that 60% of the energy produced during the winter season (here defined as the 6 coldest months of the year), and assuming that production loss caused by icing only happens in the winter season, one can estimate the production loss

$$P_{loss} = 0.6 \frac{T_{icing}}{4380\text{hr}} \qquad (2)$$

where $T_{icing}$ is the expected number of icing > 10 g/hr during a year. For the site in Nordland with 1000 hours of icing per year the production loss would be estimated to 14% using (2). This is clearly to low compared to 22% found using the timeseries of wind speed and icing. Equation (2) assumes that the cases with ice accumulation is randomly distributed throughout the winter season and is not dependent on wind speed or wind direction, while as seen in Fig. 5 this is not the case.

Clearly, exposed sites such as the one in Nordland will be related to larger losses than less exposed sites. A range for the expected production loss is given in Fig. 6. The lower boundary is given as (2). The upper boundary is given as twice the lower boundary. Sites that are more exposed to icing in the main wind direction will more typically experience production losses near the upper boundary while less exposed sites will experience losses in the lower part of the range.

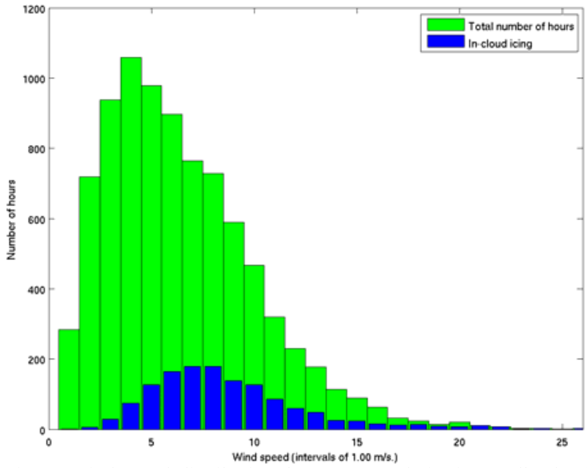


Fig. 4. Wind speed distribution for an exposed site in Nordland. The green bars represent the distribution for all data at this point. The blue bars represent the distribution in wind speed for the cases where the icing rate exceeds 10 g/hr.

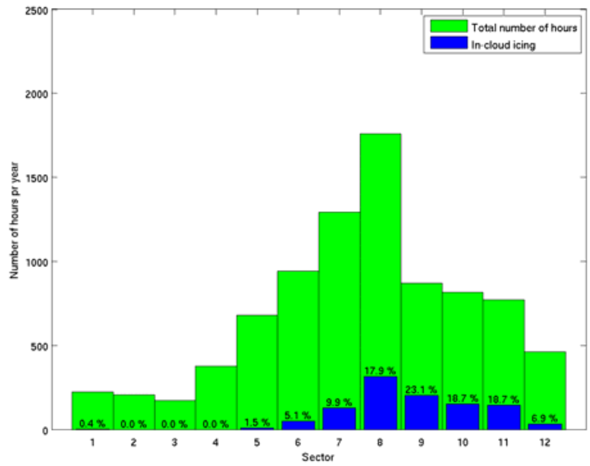


Fig. 5. Distribution of wind direction for a site in Nordland. The green bars represent the distribution for all data at this point. The blue bars represent the wind direction for the cases where the icing rate exceeds 10 g/hr. The magnitude of the blue bars relative to the green bars in is given as percentage. The distribution is given as 12 sectors, where sector 1 represents northerly wind.

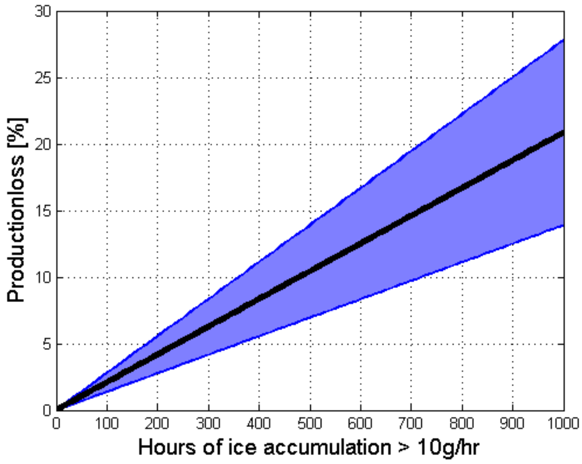


Fig. 6. Estimated range for production loss. Lower boundary is given by (2). Upper boundary is given as twice the lower boundary.

To test how well this will fit to the data from the model we calculate the production losses for a large number of grid cells for an area in Nordland where the main wind direction corresponds to large moisture supply. And we do the same calculation for another model simulation for Rogaland, which is on the southwest coast of Norway and is less exposed to icing in the main wind direction. The result for Nordland is shown in Fig. 7, while for Rogaland in Fig. 8.

For Nordland we find a number of locations where the production loss exceeds the estimated range. These are all cases with relatively modest amounts of icing (less than 500 hours). For Rogaland the occurrences of icing is in general lower than for Nordland, but the related production losses is found in the lower part of the estimated range.

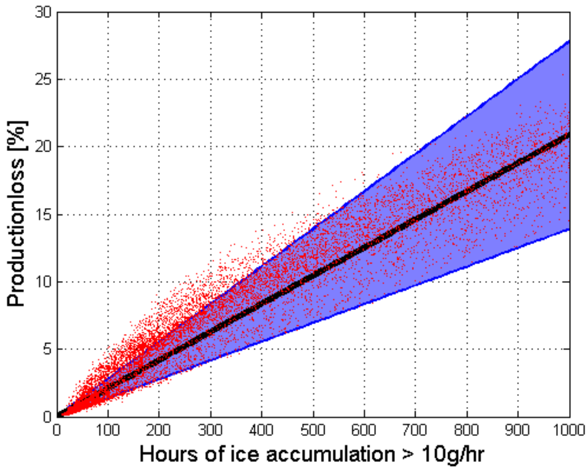


Fig. 7. Production loss estimate for Nordland. The red dots represent calculations from individual grid cells using time series of wind speed and icing.

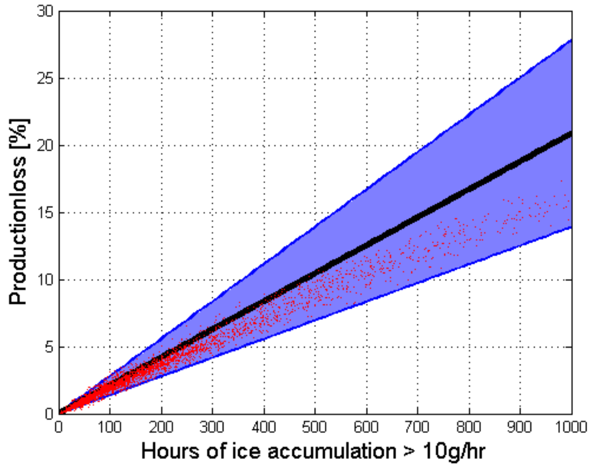


Fig. 8. Same as Fig. 7, but for Rogaland.

## V. Discussion

In this paper a simple approach to estimate production loss due to icing have been developed. The following assumptions have been made to reach an estimate:

1. An icing episode is identified when the icing rate exceeds 10g/hr. It is possible that production can continue nearly unaffected by the icing also at higher icing rate. To get a better estimate of production loss due to icing one should figure out at the icing rate limit where the production should be stopped.
2. We assume that normal production can continue after an icing episode. This implies some sort of de-icing system. If no de-icing system is installed, the ice accumulated during the event may still be present on the blades. Production may continue, but with lower output than normal as found in e.g. [8]-[9].

## VI. Summary

Icing is calculated using data from a model simulation with the meso-scale model WRF. The final result from the icing calculation is presented on a map along with a wind map of the same region. The degree of icing is found to be strongly dependent on elevation, but also to depend on wind speed and wind direction.

A simple method to estimate production loss by using the icing map has been developed. For areas in Nordland we find a tendency that icing occurs more frequently in combination with higher wind speeds than for lower wind speeds, with the result of larger production loss than for a randomly distributed sample.

## VII. Acknowledgment

The model simulation has been supported by the Norwegian Water Resource and Energy Directorate (NVE). The simulations have been performed at the linux cluster Titan at University of Oslo.

## VIII. REFERENCES


[1] E. Berge, R. E. Bredesen and K. Mollestad. “Combining WAsP with WRF meso-scale model: Evaluation of Wind Resource Assessment for three Norwegian Wind Farm Areas” in proc. EWEC 2007, Milan, Italy, 2007.

[2] E. Berge, Ø. Byrkjedal, Y. Ydersbond and D. Kindler. “Modelling of offshore wind resources. Comparison of a meso-scale model and measurements from FINO 1 and North Sea oil rigs.”, in proc. EWEC 2009, Marseille, France, March 2009.

[3] Ø. Byrkjedal and E. Berge. "Meso-scale model shows promising results in predicting icing", in proc. EWEC 2009, Marseille, France, March 2009.

[4] J. B. Klemp, W. C. Skamarock, and J. Dudhia. “Conservative split-explicit time integration methods for the compressible non-hydrostatic equations.” Available: http://www.wrf-model.org/.

[5] J. Michalakes, S. Chen, J. Dudhia, L. Hart, J. Klemp, J. Middlecoff, and W. Skamarock. “Development of a Next Generation Regional Weather Research and Forecast Model.” Developments in Teracomputing: Proceedings of the Ninth ECMWF Workshop on the Use of High Performance Computing in Meteorology 2001. Eds. Walter Zwieflhofer and Norbert Kreitz. World Scientific, Singapore. pp. 269-27.

[6] ISO standard on atmospheric icing on structures, ISO 12494, 2001.

[7] K. Harstveit, “Validation of an in-cloud icing model based on cloud water gradient calculated from metar airport data,” in the *13th Int. Workshop on Atmos. Icing of Structures*, Andermatt, Switzerland, 2009.

[8] H. Seifert and F. Richert. “A recipe to estimate aerodynamics and loads on iced rotor blades.” in proc BOREAS IV, Enontekiö, Hetta, Finland, March 1998.

[9] E Haapanen. “Influence of ice accretion on wind turbine performance.” in proc BOREAS III, Saariselkä, Finland, March 1996.